

## Original articles

Research article

<https://doi.org/10.17308/kcmf.2021.23/3533>

## Structure and chemical composition of grain boundaries in the magnetic semiconductor GaSb<Mn>

V. P. Sanygin, O. N. Pashkova, A. D. Izotov✉

*Kurnakov Institute of General and Inorganic Chemistry of the Russian Academy of Sciences,  
31 Leninsky prospekt, Moscow 119991, Russian Federation*

### Abstract

The structure and chemical composition of grain boundaries in GaSb<Mn> magnetic semiconductors have been investigated. We determined that quenching of the GaSb melt with 2% Mn results in the formation of a textured polycrystal (111). The grain boundaries of the texture are formed by split 60 degree dislocations with <110> dislocation lines. Microinclusions based on the ferromagnetic compound MnSb are located on the stacking faults of split dislocations. The chemical compositions of microinclusions differ, but their average composition is close to Mn<sub>1.1</sub>Sb. The synthesized GaSb<Mn> is a soft ferromagnet with a coercive force of 10 Oe and a magnetic state approaching superparamagnetic.

**Keywords:** Magnetic semiconductors, Gallium antimonide, Crystal lattice defects, Magnetic clusters

**Acknowledgements:** The work was supported by the Ministry of Education and Science of the Russian Federation within the framework of the state order to Kurnakov Institute of General and Inorganic Chemistry of the Russian Academy of Sciences. The authors are grateful to the Centre for Collective Use of Physical Research Methods of IGIC RAS.

**For citation:** Sanygin V. P., Pashkova O. N., Izotov A. D. Structure and chemical composition of grain boundaries in the magnetic semiconductor GaSb<Mn>. *Kondensirovannye sredy i mezhfaznye granitsy = Condensed Matter and Interphases*. 2021;23(3): 413–420. <https://doi.org/10.17308/kcmf.2021.23/3533>

**Для цитирования:** Саныгин В. П., Пашкова О. Н., Изотов А. Д. Структура и химический состав межзеренных границ в магнитном полупроводнике GaSb<Mn>. *Конденсированные среды и межфазные границы*. 2021;23(3): 413–420. <https://doi.org/10.17308/kcmf.2021.23/3533>

✉ Alexander D. Izotov, e-mail: [izotov@igic.ras.ru](mailto:izotov@igic.ras.ru)

© Sanygin V. P., Pashkova O. N., Izotov A. D., 2021



## 1. Introduction

The production of spintronic devices requires materials that have both magnetic and semiconductor properties and are technologically compatible with common semiconductor devices. Recently, a large number of studies have focused on the search for new magnetic semiconductors in the form of solid solutions of manganese in III–V compounds, i.e. dilute magnetic semiconductors (DMS) [1].

All these studies employed the latest technologies, including molecular-beam epitaxy (MBE), laser irradiation, ion implantation, etc. Nevertheless, they did not manage to overcome the low solubility limit of manganese, because, according to the results of the studies, at room temperature and above ferromagnetism of  $A^{III}B^V$  is explained by the formation of microinclusions based on Mn–V magnetic compounds [2–16].

At the same time, cluster magnetic semiconductors have certain advantages over dilute magnetic semiconductors. These materials are of practical importance since it is possible to control their magnetic properties by modifying the composition, the size, and the concentration of the forming magnetic microinclusions without using expensive technologies.

It is important to perform a comprehensive study of the effect of rapid melt crystallisation on the composition, structure, and properties of Mn-doped gallium antimonide. The article presents the results of the study of the structure and chemical composition of grain boundaries in GaSb<Mn> obtained by melt quenching.

## 2. Experimental

In order to obtain bulk samples of GaSb+2% Mn we used the following initial components: hole-conducting monocrystalline gallium antimonide and pure Mn (99.99%). The samples were prepared by melting the mixture in a vacuum quartz ampoule at  $T = 1200$  K, incubating the melt at this temperature for 24 hours, and the following vertical quenching of the melt in a mixture of water and ice.

The samples were identified using X-ray phase analysis (XRD), performed using a BRUKER D8 ADVANCE diffractometer ( $\text{CuK}_\alpha$ -radiation) at the Centre for Collective Use of Physical Research Methods of the Kurnakov Institute of

General and Inorganic Chemistry of the Russian Academy of Sciences (CCU IGIC RAS). The angle range  $2\theta$  was from  $10^\circ$  to  $80^\circ$  with the scanning step  $\Delta 2\theta = 0.014^\circ$ . The XRD patterns were then analysed using the ICDD PDF-2 database.

The section surface was studied by means of scanning electron microscopy (SEM). Micrographs and chemical compositions of certain phases on the microstructure level were obtained at CCU IGIC RAS using a Carl Zeiss Nvision40 scanning electron microscope with an Oxford Instruments X-Max microprobe analyser.

The magnetic properties of the GaSb(2 % Mn) samples were studied at  $T = 4$  K and  $T = 300$  K in a magnetic field of up to  $H = 50$  kOe using a PPMS-9 (Quantum Design) automated measurement system. When measuring the DC magnetization the absolute sensitivity was  $\pm 2.5 \cdot 10^{-5}$  g/cm<sup>3</sup>.

## 3. Results and discussion

In [16], we suggested that dislocations in semiconductors doped with magnetic impurities can be used as extensive linear magnetic circuits aligned in the same crystallographic direction. The concept of impurity-dislocation magnetism was inspired by the studies of the Cottrell atmosphere formation [17] and spheroid formation [18] performed by means of 3D imaging of impurity segregation near dislocations inside a crystal.

It was demonstrated that the impurity segregation in dislocations by means of atom diffusion inside the crystal is as intensive as the impurity segregation by means of decorating the dislocations on the surface. Therefore, we conducted a series of experiments, where III–V semiconductor compounds were doped with a *d*-element – manganese.

Namely, we analysed the samples of the semiconductor compound GaSb doped with 2 at% Mn.

Identically aligned dislocations were generated by quenching the melt at different coefficients of linear thermal expansion for GaSb ( $\alpha \approx 6.7 \cdot 10^{-6}$  K<sup>-1</sup> [19]) and quartz ( $\alpha \approx 0.5 \cdot 10^{-6}$  K<sup>-1</sup> [20]), with heat being removed radially from the cylindrical part of the melt-containing ampoule during the vertical quenching (Fig. 1a). Judging by the temperature dependence of the magnetization, the samples were ferromagnets with a Curie temperature  $T_c = \sim 560$  K (Fig. 1b).

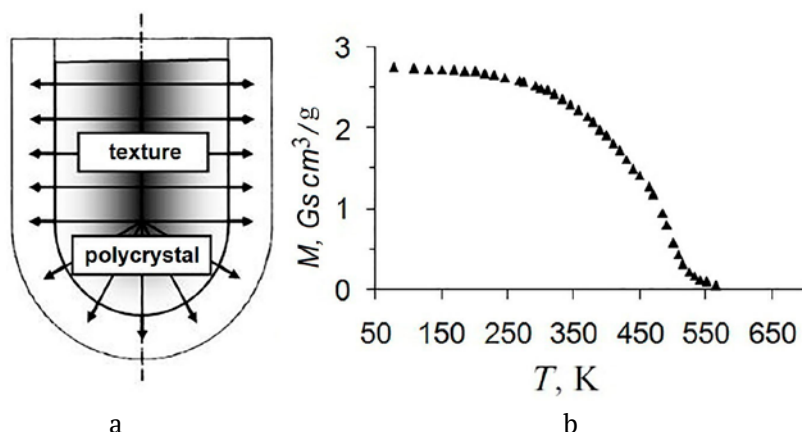


**Fig. 1.** Diagram of an ampoule with the melt placed vertically during quenching (a) and the temperature dependence of the specific magnetization of the sample of GaSb + 2 % Mn (b)

Fig. 2a demonstrates a diffraction pattern of the synthesised GaSb<Mn> powder. Besides the peaks of polycrystalline GaSb, it shows peaks of the ferromagnetic compound  $Mn_{1,1}Sb$  whose Curie temperature complies with the magnetic properties of the sample (Fig. 1b).

In order to further study the structural properties of the material, we produced a metallographic thin section of its ingot, whose diffraction pattern is given in Fig. 2b. It shows that the metallographic thin section of GaSb<Mn> is a texture, and therefore consists of blocks separated by low-angle grain boundaries formed by dislocations.

The (111) texture axis indicates that the dislocations controlling the grain formation

are 60 degree edge dislocations with the (111) slip plane and the dislocation line <110>, which contradicts the generally accepted view that the structure of the sphalerite is formed by Lomer dislocations with (110) slip planes.

In order to see whether Lomer dislocations participate in the formation of the texture we synthesised a sample of a different III–V compound (InSb) by means of melt quenching. The diffraction pattern of the InSb powder is given in Fig. 2c. It demonstrated InSb peaks with the crystal structure of sphalerite type, identical to GaSb. However, the diffraction pattern of the crystallographic thin section of InSb corresponds to the texture with simple slip planes of type (110),

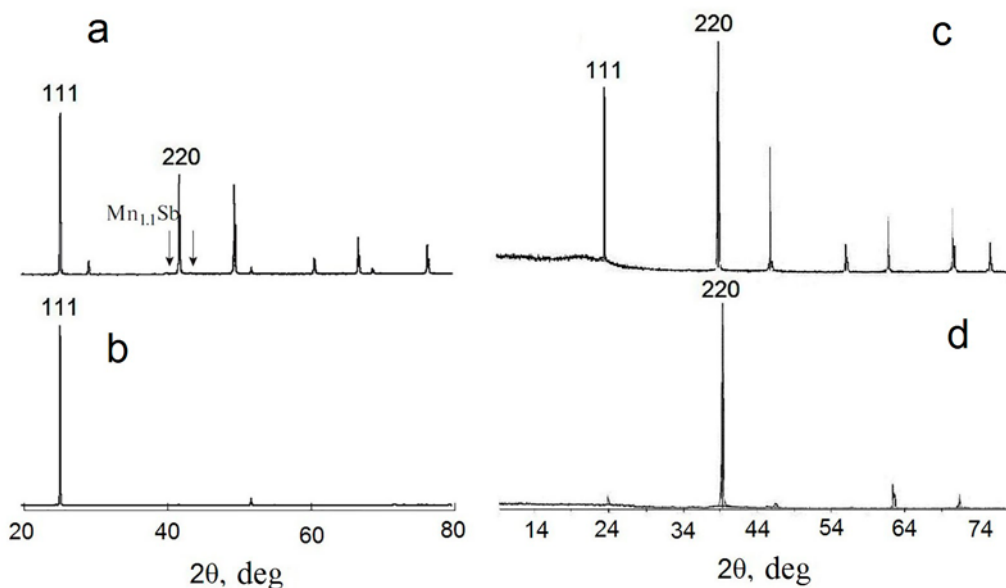


**Fig. 2.** X-ray diffraction patterns of (a) powder and (b) metallographic thin section of GaSb doped with Mn; powder (c) and metallographic thin section (d) of undoped InSb

which agrees well with the existing concepts.

Thus, in our study, we determined that the introduction of impurities during the melt quenching affects the orientation of the resulting ingots of III-V semiconductor compounds. To explain this phenomenon, let's consider the formation of a Lomer sessile dislocation.

Fig. 3a shows a simple 60 degree edge dislocation most common for a crystal structure of sphalerite type. Such dislocations are characterised by a (111) slip plane of the dislocation line along the crystallographic direction  $\langle 110 \rangle$ ; the family of the direction in the structure of the sphalerite is shown in Fig. 3b.

According to [21, 22], the formation of the Lomer sessile dislocation is a complex process including the following states of the material:

1 – formation of 60 degree edge dislocations in intersecting crystallographic planes;

2 – splitting of the edge dislocations into 30 and 90 degree dislocations, connected by a layer of stacking faults with two stacking faults moving towards each other until they meet at the planes intersection (Fig. 3b);

3 – formation of the Lomer sessile dislocation (Fig. 3c).

The possibility of all the stages taking place is quite high in pure semiconductors with a sphalerite structure. However, when an impurity is added to the crystal, the regions of hydrostatic compression and expansion around the extra half-plane of the edge dislocation begin to play a significant role. In Fig. 3a the region of hydrostatic compression is shaded. The impurity atoms intensively diffuse towards the regions of arising stresses, segregate around the extra half-plane, pin the dislocations to the crystal lattice of the material, and immobilise them.

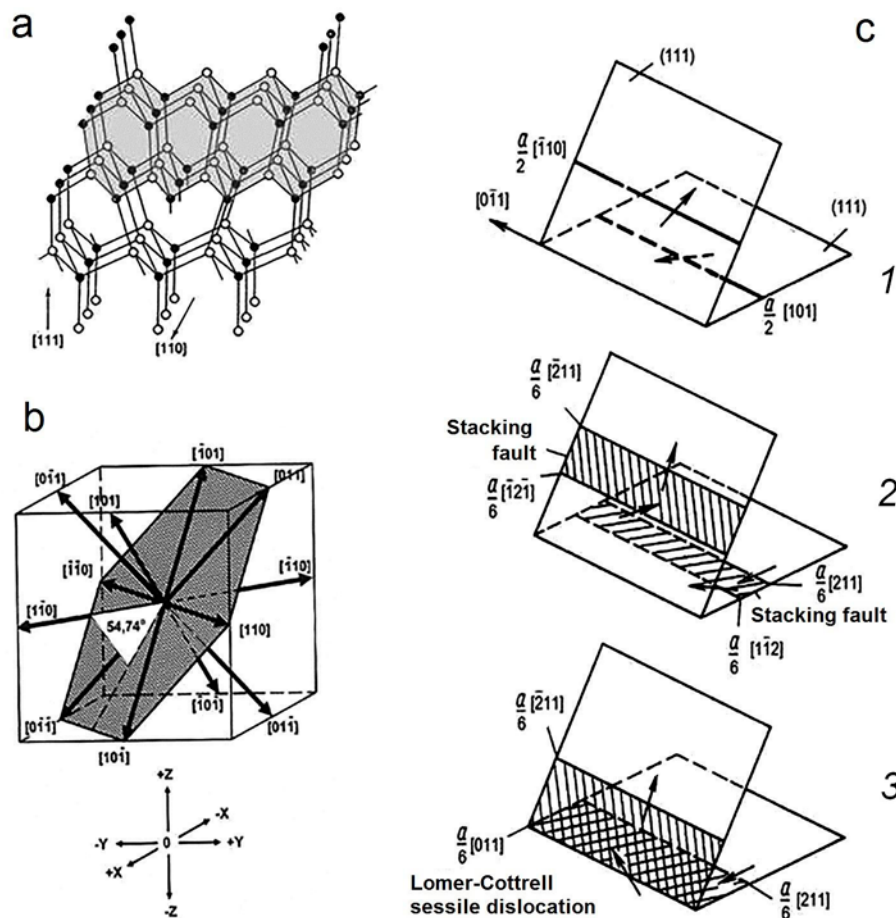


**Fig. 3.** Edge dislocation and Lomer sessile dislocation: a – initial 60 degree dislocation of GaSb with a shaded region of hydrostatic compression and a [110] dislocation line; b – the family of [110] directions in the sphalerite structure; c – a diagram of the formation of the Lomer sessile dislocation

If the diffusion rate is higher than the rate of formation of sessile dislocations, the latter do not appear. This is what happens when GaSb is doped with manganese. Of the two ways to hinder the dislocation motion, segregation of the impurity is the main one, and therefore the third stage of the formation of sessile dislocations does not occur.

Fig. 4a demonstrates a scheme and Fig. 4b shows the result of scanning electron microscopy of split dislocations of the surface of GaSb doped with Mn.

A split dislocation has the form of a stacking fault ribbon bounded by partial dislocations. The stretching of the stacking fault aims to pull the partial dislocations together, while pressing the microimpurities located between them (Fig. 4b), and limit their size.

The stacking fault ribbon is a two-dimensional crystal interlayer with incorrect alterations of the atomic close-packed layers of the FCC lattice and the formation of a thin interlayer of the

hexagonal close-packed (HCP) structure. The split dislocation may consist of three, four, or more partial dislocations, and therefore of two, three, or more stacking fault ribbons, and come in the form of alternating regions of FCC and HCP lattices.

To determine the chemical composition of grain boundaries in GaSb<Mn>, we studied the chemical composition of the microinclusions on the dislocations controlling the grain formation by means of electron probe microanalysis. Since the region of X-ray excitation by an electronic probe is about 1 μm, we studied the inclusions of 1 μm size separated and surrounded by a relatively smooth surface of the semiconductor (Fig. 5a). We estimated the accuracy of identification to be ±2 at%.

The parameters of the chemical composition of the microinclusions were placed on the composition line of the state diagram Mn–Sb [23] (Fig. 5b). Then we performed phase identification

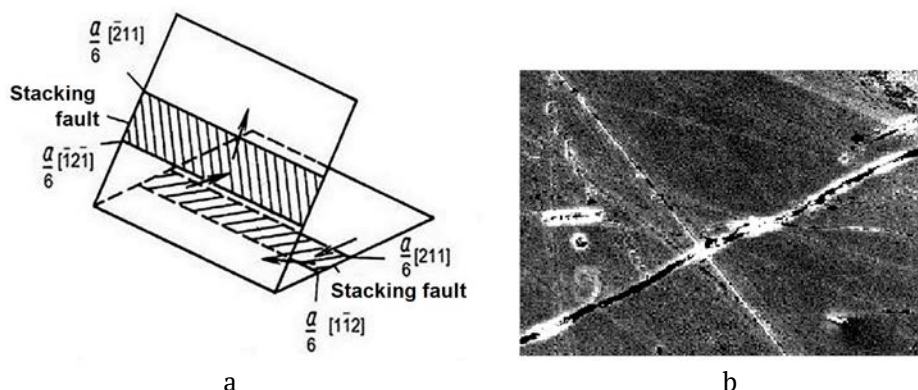


Fig. 4. Scheme (a) and SEM images (b) of split dislocations on the surface of GaSb doped with manganese

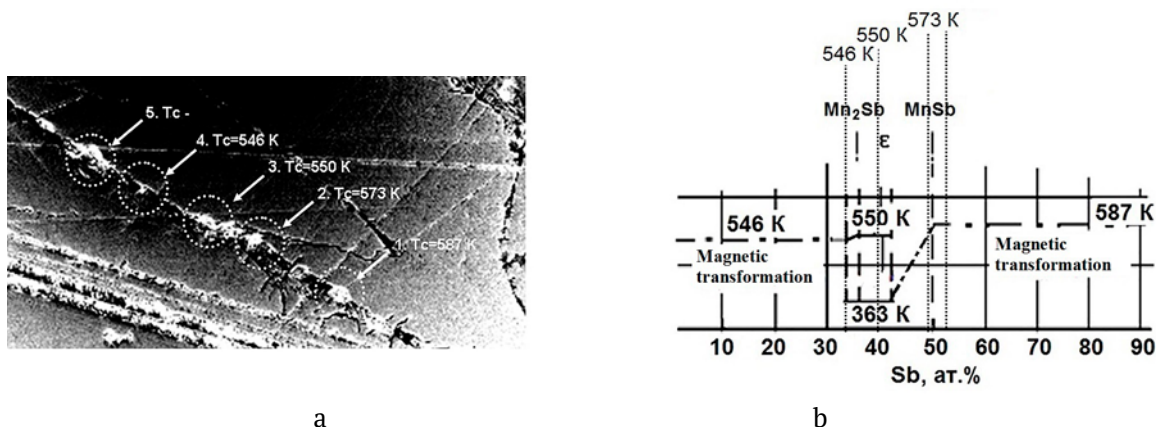


Fig. 5. Dislocation outcrops on the surface of GaSb doped with Mn (a) and their compositions on the lines of magnetic transformations of the Mn-Sb phase diagram (b)



of the microinclusions and determined the type of magnetism and the Curie temperature for each of them. Fig. 5b shows that, although the chemical compositions of the microinclusions differ, their average composition is close to  $Mn_{1.1}Sb$ . The difference in the compositions is caused by the difference in the cooling rate during directional crystallisation of the melt from the surface to the centre of the ingot (in Fig. 1a the process is indicated by the gradual change in the contrast of the melt).

The temperature dependence of zero field cooled (ZFC) and field cooled (FC) magnetization of the  $GaSb<Mn>$  texture was the same at the cooling  $T \approx 300$  K. This means that at temperatures above room temperature the ferromagnetic state is transformed into a superparamagnetic state, and  $T \approx 300$  K is the blocking temperature for the ferromagnetic state of the texture.

Using the Bean–Livingston method [24] we can determine the dependency between

the constant of the magnetic crystallographic anisotropy, the blocking temperature and the size of single-domain microinclusions in the diamagnetic matrix of  $GaSb$ .

Assuming that magnetic clusters are spherical, the maximum radius of the blocked effective clusters is about 180–200 nm.

Thus, the calculated maximum effective size of the blocked clusters  $r \approx 200$  nm is close to the micron size of magnetic inclusions in dislocations (Fig. 4b).

The study of the magnetic properties demonstrated that at the temperature  $T = 300$  K, sample  $GaSb<Mn>$  is still a ferromagnet with the coercive force of a soft magnetic material  $H_c \approx 10$  Oe (Fig. 6).

The dislocation lines doped with magnetic impurities in a diamagnetic semiconductor matrix are artificially induced easy axes of magnetization. The magnetic moments of single-domain particles can be located along  $\langle 110 \rangle$  or

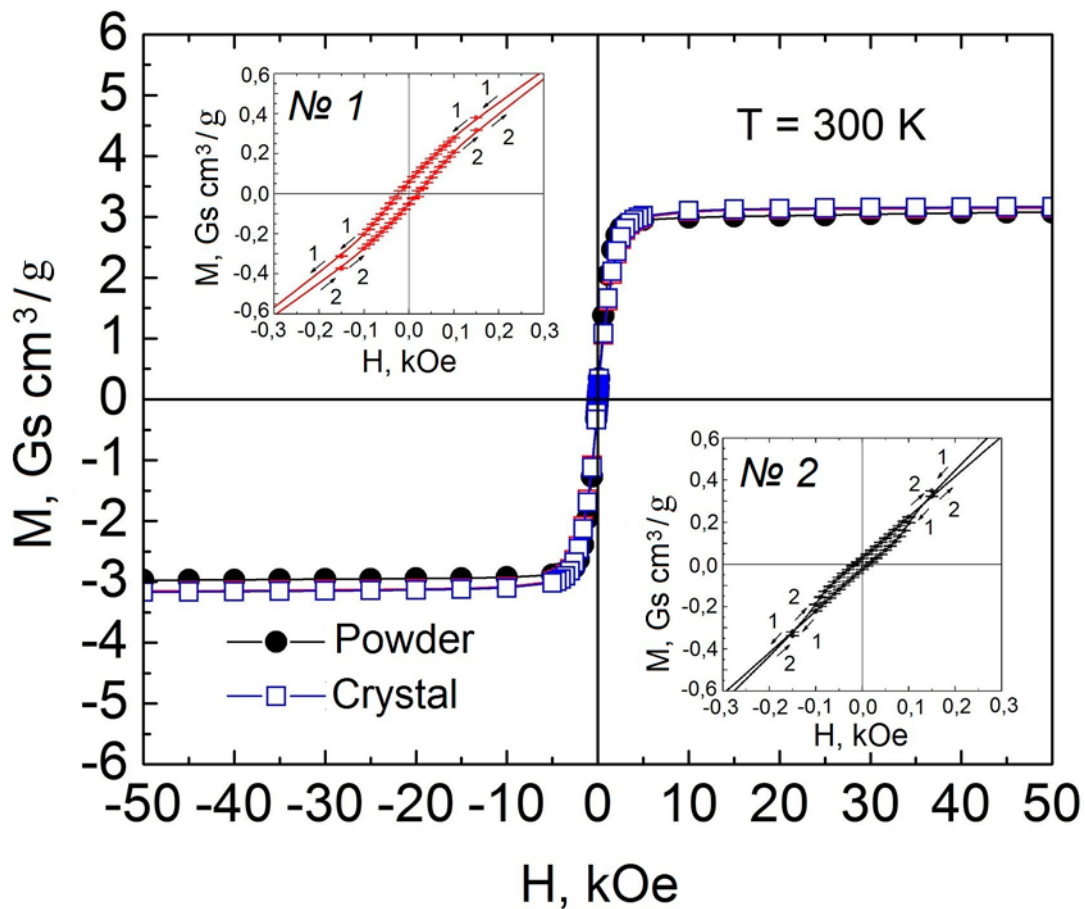


**Fig. 6.** Field dependences of the magnetization of the crystal and powder of  $GaSb$  doped with  $Mn$ . Inserts: No.1: the hysteresis loop region of the crystal, No.2: the hysteresis loop region of the powder

<-1-10> directions depending on the direction of the external magnetic field  $+H$  or  $-H$ . (Fig. 3b).

The characteristic feature of superparamagnetism is the merging of the demagnetization and magnetization curves, which means that hysteresis disappears. In this regard, it is interesting to compare the demagnetization and magnetization curves of the texture and its powder in the vicinity of a zero magnetic field. While the texture still has ferromagnetic properties (insert No.1, Fig. 6), in the case of its powder (insert No.2, Fig. 6) demagnetization and magnetization curves change places in the regions of magnetic tension  $H = \pm 0.15$  kOe. With the magnetic tension being from  $-0.15$  to  $+0.15$  kOe, both curves merge (taking into account the measurement error) and form a region of superparamagnetic state.

#### 4. Conclusions

As a result of our study we obtained samples of a semiconductor compound GaSb+2 at% Mn.

XRD analysis demonstrated that the main source of ferromagnetism in the obtained samples is the  $Mn_{1-x}Sb_x$  phase with the Curie temperature  $T_C = \sim 560$  K. The study also demonstrated the fundamental importance of the heat removal mode during the process of melt crystallisation and explained the formation of the <111> texture in GaSb that has a sphalerite crystal structure. We also determined that grain boundaries are formed by split edge dislocations.

SEM was used to determine the chemical compositions of microinclusions in stacking faults of split dislocations, perform their phase identification, and determine the type of magnetism and the Curie temperature for each of them.

The study of the magnetic properties showed that quenching of bulky samples of GaSb<Mn> results in the formation of a soft magnetic material. It also demonstrated the possibility of transition from the ferromagnetic to the superparamagnetic state.

#### Author contributions

All authors made an equivalent contribution to the preparation of the publication.

#### Conflict of interests

The authors declare that they have no known competing financial interests or personal

relationships that could have influenced the work reported in this paper.

#### References

1. Ivanov V. A., Aminov T. G., Novotortsev V. M., Kalinnikov V. T. Spintronics and spintronics materials. *Russian Chemical Bulletin*. 2004;53(11): 2357-2405. <https://doi.org/10.1007/s11172-005-0135-5>
2. Pulzara-Mora C., Pulzara-Mora A., Forero-Pico A., Ayerbe-Samaca M., Marques-Marchan J., Asenjo A., Nemes, N. M., Arenas D., Saez Puche R. Structural, morphological and magnetic properties of GaSbMn/Si(111) thin films prepared by radio frequency magnetron sputtering. *Thin Solid Films*. 2020;705: 137971. <https://doi.org/10.1016/j.tsf.2020.137971>
3. Dmitriev A. I., Kochura A. V., Kuz'menko A. P., Parshina L. S., Novodvorskiy O. A., Khranova O. D., Kochura E. P., Vasil'ev A. L., Aronzon B. A. Effect of Heat Treatment on the Dispersion of the Magnetic Anisotropy of MnSb Nano-inclusions Embedded in Thin GaMnSb Films. *Physics of the Solid State*. 2019;61(4): 523–529. <https://doi.org/10.1134/S1063783419040073>
4. Doria-Andrade J., Pulzara-Mora C., Bernal-Correa R., Rosales-Rivera A., Pulzara-Mora A. Segregation of Mn into GaAsMn thin films prepared by magnetron sputtering. *Materia-Rio De Janeiro*. 2020;25(4): E-12884. <https://doi.org/10.1590/s1517-707620200004.1184>
5. Yokoyama M., Ogawa T., Nazmul A. M., Tanaka M. Large magnetoresistance (> 600 %) of a GaAs : MnAs granular thin film at room temperature *Journal of Applied Physics*. 2006;99(8): 08D502. <https://doi.org/10.1063/1.2151817>
6. Rednic L., Deac I. G., Dorolti E., Coldea M., Rednic V., Neumann M. Magnetic cluster development in  $In_{1-x}Mn_xSb$  semiconductor alloys. *Open Physics*. 2010;8(4): 620–627. <https://doi.org/10.2478/s11534-009-0140-7>
7. Tran L., Hatami F., Masselink W. T., Herfort J., Trampert A. Distribution of Mn in ferromagnetic (In,Mn)Sb films grown on (0 0 1) GaAs using MBE. *Journal of Crystal Growth*. 2011;323(1): SI 340–343 (Special Issue). <https://doi.org/10.1016/j.jcrysgro.2010.10.127>
8. Overberg M. E., Gila B. P., Thaler G. T., Abernathy C. R., Pearton S. J., Theodoropoulou N. A. et. al. Room temperature magnetism in GaMnP produced by both ion implantation and molecular-beam epitaxy. *Journal of Vacuum Science & Technology B: Microelectronics and Nanometer Structures*. 2002; 20(3): 969–973. <https://doi.org/10.1116/1.1477424>
9. Sobolev N. A., Oliveira M. A., Rubinger R. M., Neves A. J., Carmo M. C., Lesnikov V. P., Podolskii V. V., Danilov Y. A., Demidov E. S., Kakazei G. N. Ferromagnetic resonance and Hall effect characterization of GaMnSb

layers. *Journal of Superconductivity and Novel Magnetism*. 2007;20(6): 399–403. <https://doi.org/10.1007/s10948-007-0243-6>

10. Hartmann Th., Lampalzer M., Klar P. J., Stolz W., Heimbrodt W., von Nidda H. A. K., Loidl A., Svistov L. Ferromagnetic resonance studies of (Ga,Mn)As with MnAs clusters. *Physica E: Low-dimensional Systems and Nanostructures*. 2002;13(2-4): 572–576. [https://doi.org/10.1016/s1386-9477\(02\)00180-7](https://doi.org/10.1016/s1386-9477(02)00180-7)

11. Chen C., Chen N., Liu L., Li Y., Wu J. Ga<sub>1-x</sub>Mn<sub>x</sub>Sb grown on GaSb substrate by liquid phase epitaxy. *Journal of Crystal Growth*. 2004;260(1-2): 50–53. <https://doi.org/10.1016/j.jcrysgro.2003.08.022>

12. Yoshizawa H., Toyota H., Nakamura S., Yamazaki M., Uchitomi N. Structural and ferromagnetic properties of InMnAs thin films including MnAs nanoclusters grown on InP substrates. *Thin Solid Films*. 2017;622: 136–141. <https://doi.org/10.1016/j.tsf.2016.12.020>

13. Novak J., Dujavova A., Vavra I., Hasenoehrl S., Reiffers M. Magnetic properties of InMnAs nanodots prepared by MOVPE. *Journal of Magnetism and Magnetic Materials*. 2013;327: 20–23. <https://doi.org/10.1016/j.jmmm.2012.09.041>

14. Liu J. D., Hanson M. P., Peters J. A., Wessels B. W. Magnetism and Mn Clustering in (In,Mn)Sb magnetic semiconductors. *ACS Applied Materials & Interfaces*. 2015;7(43): 24159–24167. <https://doi.org/10.1021/acsami.5b07471>

15. Yakovleva E. I., Oveshnikov L. N., Kochura A. V., Lisunov K. G., Lahderanta E., Aronzon B. A. Anomalous Hall effect in the In<sub>1-x</sub>Mn<sub>(x)</sub>Sb dilute magnetic semiconductor with MnSb inclusions. *JETP Letters*. 2015;101(2): 130–135. <https://doi.org/10.1134/s0021364015020149>

16. Sanygin V. P., Tishchenko E. A., Shi D. H., Izotov A. D. Concept of impurity-dislocation magnetism in III-V compound semiconductors. *Inorganic Materials*. 2013;49(1): 6–13. <https://doi.org/10.1134/s0020168513010147>

17. Blavette D., Cadel E., Fraczkiewicz A., Menand A. Three-dimensional atomic-scale imaging of impurity to line defects. *Science*. 1999;286(5448): 2317–2319. <https://doi.org/10.1126/science.286.5448.2317>

18. Nechaev Yu. S. Metallic materials for the hydrogen energy industry and main gas pipelines: complex physical problems of aging, embrittlement, and failure. *Physics-Uspekhi*. 2008;51(7): 681–697. <https://doi.org/10.1070/pu2008v051n07abeh006570>

19. Strel'chenko S. S., Lebedev V. V. *Soedineniya A<sup>3</sup>B<sup>5</sup>* [Compounds A<sup>3</sup>B<sup>5</sup>] Moscow: Metallurgiya Publ.; 1984. 144 p. (In Russ.)

20. *Fizicheskie velichiny*. Spravochnik pod redaktsiei Grigor'eva I. S., Meilikhova E. Z. [Physical quantities. Handbook. I. S. Grigoriev, E.Z. Meilikhov (eds.)]. Moscow: Energoatomizdat Publ.; 1991. 1232 p. (In Russ.)

21. Osip'yan Yu. A. *Elektronnyye svoystva dislokatsii v poluprovodnikakh* [Electronic properties of dislocations in semiconductors.]. Moscow: Editorial URSS Publ.; 2000. 314 p. (In Russ.)

22. Hull D. *Introduction to dislocations*. Oxford, New York: Pergamon Press; 1984. 257 p.

23. *Diagrammy sostoyaniya dvoynykh metallicheskih sistem: Spravochnik: v 3 t. Kn. 1* [State diagrams of double metal systems: Handbook: In 3 vols. Book 1] / N. P. Lyakisheva (ed.). Moscow: Mashinostroenie Publ.; 2001. 872 p. (In Russ.)

24. Bean C. P., Livingston J. D. Superparamagnetism. *Journal of Applied Physics* 1959;30: S120. <https://doi.org/10.1063/1.2185850>

### Information about the authors

*Vladimir P. Sanygin*, PhD in Chemistry, senior research fellow, Laboratory of Semiconductor and Dielectric Materials, Kurnakov Institute of General and Inorganic Chemistry of the Russian Academy of Sciences, Moscow, Russian Federation; e-mail: [sanygin@igic.ras.ru](mailto:sanygin@igic.ras.ru). ORCID iD: <https://orcid.org/0000-0002-1261-6895>.

*Olga N. Pashkova*, PhD in Chemistry, senior research fellow, Laboratory of Semiconductor and Dielectric Materials, Kurnakov Institute of General and Inorganic Chemistry of the Russian Academy of Sciences, Moscow, Russian Federation; e-mail: [olg-pashkova@yandex.ru](mailto:olg-pashkova@yandex.ru). ORCID iD: <https://orcid.org/0000-0002-2102-1025>.

*Alexander D. Izotov*, DSc in Chemistry, Associate Member of the Russian Academy of Sciences, Chief Researcher, Laboratory of Semiconductor and Dielectric Materials, Kurnakov Institute of General and Inorganic Chemistry of the Russian Academy of Sciences, Moscow, Russian Federation; e-mail: [izotov@igic.ras.ru](mailto:izotov@igic.ras.ru). ORCID iD: <https://orcid.org/0000-0002-4639-3415>.

Received 14 April 2021; Approved after reviewing 30 April 2021; Accepted for publication 15 May 2021; Published online 25.09.2021.

Translated by Yulia Dymant

Edited and proofread by Simon Cox